Journal of Materials Chemistry B

RSC Publishing

PAPER

View Article Online
View Journal | View Issue

Cite this: J. Mater. Chem. B, 2013, 1, 1909

Impact of mesoporous silica nanoparticle surface functionality on hemolytic activity, thrombogenicity and non-specific protein adsorption†

Adem Yildirim,[ab] Erol Ozgur[ab] and Mehmet Bayindir*[abc]

Although numerous mesoporous silica nanoparticle (MSN) drug carriers and theranostic agents with various surface functionalities have been designed in the last decade, their biocompatibility remains a matter of intensive debate. Here, we systematically evaluated interactions of a series of MSNs possessing different surface functional groups (ionic, polar, neutral, and hydrophobic) with blood constituents, in terms of their hemolytic activity, thrombogenicity, and adsorption of blood proteins on their surfaces. Using a hemolysis assay we showed that surface functionalization can reduce or even completely prevent the hemolytic activity of bare MSNs. We investigated thrombogenicity of MSNs by measuring prothrombin time (PT) and activated partial thromboplastin time (aPTT). We observed that none of the MSNs used in this study exhibit significant thrombogenic activity. Lastly, we examined non-specific protein adsorption on MSN surfaces using human serum albumin (HSA) and gamma globulins (γGs) and found that surface functionalization with ionic groups can greatly reduce protein adsorption. Demonstration of the surface functionalization having a crucial impact on blood compatibility might serve as a guideline for further investigation related to the design of mesoporous silica systems for biomedical applications, and shed light on research towards the ultimate goal of developing smart theranostic systems.

Received 17th November 2012
Accepted 1st February 2013

DOI: 10.1039/c3tb20139b

www.rsc.org/MaterialsB

Introduction

Extensive research on mesoporous silica nanoparticles in the last decade has shown the promising potential of these materials in biomedical applications as drug and gene carriers,[1–5] cell markers[6–9] and diagnostic and therapeutic agents.[10–13] However, most of the research focused on synthesis and applications of these materials and only a few reports investigated *in vitro* and *in vivo* toxicity of the MSNs. *In vitro* studies[14–16] showed good biocompatibility of mesoporous silica nanoparticles with various cell lines; nevertheless, low *in vitro* cytotoxicity does not assure that MSNs are biocompatible *in vivo*. In fact, recent reports indicate possible *in vivo* cytotoxicity of silica based materials. Several groups reported that silica and mesoporous silica nanoparticles can cause lysis of red blood cells (RBCs).[17–22] In addition, it was reported that intravenous injection of mesoporous silica particles to mice can be fatal due to the obstruction in the vasculature, which may lead to multiple subsequent vital organ failure.[23,24] In another study, silica nanoparticles were observed to cause pregnancy complications in mice.[25] These results revealed that in order to use MSNs in biological applications, their biocompatibility must be well characterized and improved to an appropriate level.

Interaction of nanoparticles with blood constituents deserves particular consideration, since the initial encounter between MSNs and the organism occurs within the circulatory system. Therefore, determining the blood compatibility of MSNs is the primary screening for their *in vivo* toxicity regarding applications where particles are delivered by intravenous injection. Nanoparticles injected into the blood may cause several adverse effects such as hemolysis and blood clot formation (thrombogenicity).[26] Hemolysis is the disintegration of RBCs due to deformation of their cell membrane. MSNs can interact with the positively charged RBC membrane electrostatically through their negatively charged surface silanol groups; therefore they can cause hemolysis.[18] Lin and Haynes[20] studied the hemolytic activity of several MSNs with diameters between 25 and 225 nm and concluded that increasing the particle size of MSNs diminished the hemolytic activity to a degree. Also, Yu *et al.*[22] demonstrated that rod shaped MSNs resulted in lower hemolytic activity than spherical ones. Nevertheless, for all cases bare MSNs cause significant hemolysis, especially at high concentrations. Blood clot formation occurs during hemostasis to stop bleeding from damaged blood vessels. Some negatively charged porous materials, such as mesoporous silica and zeolites, can accelerate the hemostasis of the blood by activation of a coagulation cascade.[27–29] Similarly,

[a]UNAM-National Nanotechnology Research Center, Turkey
[b]Institute of Materials Science and Nanotechnology, Turkey
[c]Department of Physics, Bilkent University, 06800 Ankara, Turkey. E-mail: bayindir@nano.org.tr

† Electronic supplementary information (ESI) available. See DOI: 10.1039/c3tb20139b

when MSNs are injected into the blood, they can induce clotting inside blood vessels, which can cause adverse effects, by partially or completely blocking the blood vessels, leading to stroke and death.[30–32] Therefore, in order to use MSNs safely in biological applications, thrombogenicity of these materials should be determined. Another blood nanoparticle interaction to be considered before intravenous injection of the MSNs is non-specific protein adsorption, because it can promote phagocytosis by making the nanoparticles visible to phagocytic cells. This results in rapid clearance of nanoparticles from the blood stream before they reach the target site and decreases the efficiency of applications.[33,34]

All of the above mentioned blood compatibility issues are closely related to the surfaces of the nanoparticles. Consequently, by engineering their surfaces, hemolytic activity, thrombogenicity and non-specific protein adsorption of MSNs can be depressed or eliminated. Although there are some reports demonstrating the modification of MSN surfaces with organic molecules, in particular polyethylene glycol (PEG), which can decrease hemolysis,[19,20] thrombogenicity[35] and non-specific protein adsorption,[36] to our knowledge, there is no study that systematically investigates the surface effects on blood compatibility issues of MSNs. The aim of this study is to evaluate the effects of MSN surface composition on the interaction of these particles with blood constituents (Scheme 1). Accordingly, we prepared five organosilane functionalized MSNs and an equivalent non-functionalized MSN. We also prepared Rhodamine B dye conjugated MSNs to evaluate the effect of fluorescent tagging on blood compatibility of MSNs. In addition, we prepared a PEGylated MSN in order to compare our results with a prevalent and well-characterized surface. Besides surface composition, particle size, shape and porosity can also affect the interactions of MSNs with biological systems. Therefore, in this study the particle size (around 80 nm), shape (spherical) and pore structure (hexagonally ordered 2–3 nm in size) of particles were kept constant, while their surfaces were differently functionalized. We selected a particle size of around 80 nm because it was reported that around this particle size cellular uptake is maximum for MSNs[37] and also, it is well known that particles with sizes larger than 100 nm are rapidly cleared from the blood by the reticuloendothelial system.[20] We selected the surface functional groups by considering two characteristics: (i) all surface functional groups were selected from previously used ones in MSN synthesis for different purposes such as controlling the cargo loading and release properties,[38] fluorescent tagging,[39] and improving the dispersibility of particles in biological media[6] and (ii) we select them to obtain a library of surface functionalities that covers diverse surface properties, such as anionic, cationic, neutral, hydrophobic or polar. To evaluate the blood compatibility of these MSNs, we examined hemolytic activity, thrombogenicity, and non-specific protein adsorption to their surfaces in a broad concentration range. The systematic evaluation of surface effects on blood compatibility of MSNs performed in this work can provide important insights into the rational design of mesoporous silica systems for biomedical applications.

Experimental section

Materials

Tetraethyl orthosilicate (TEOS), aminopropyltriethoxysilane (APTES), methyltrimethoxysilane (MTMS), phenyltriethoxysilane (PTES), sodium hydroxide, ammonium nitrate, Rhodamine B, *N*-(3-dimethylaminopropyl)-*N*′-ethylcarbodiimide hydrochloride

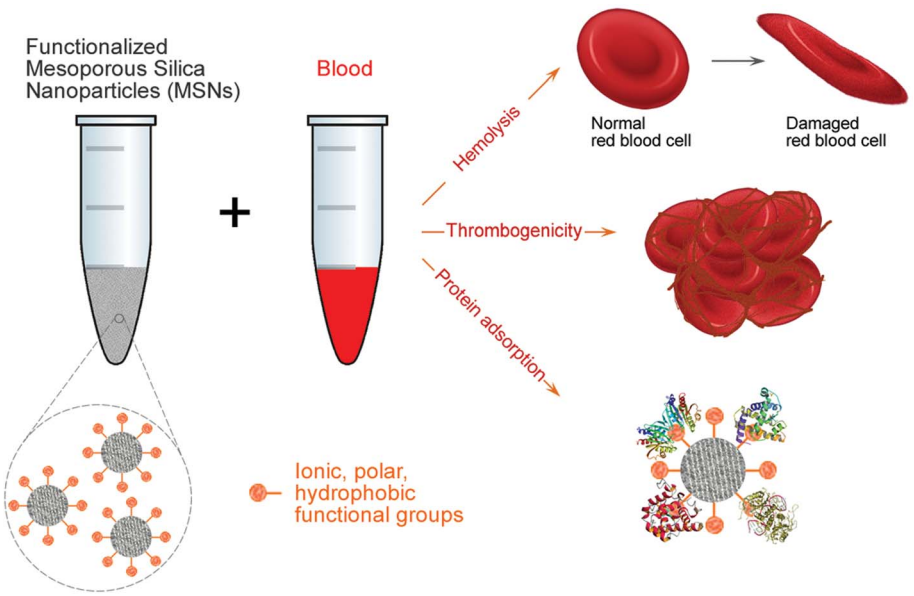

Scheme 1 Schematic representation of certain interactions between mesoporous silica nanoparticles (MSNs) and blood constituents. Surfaces of MSNs were functionalized with ionic, polar, neutral or hydrophobic organosilane monomers to evaluate the effect of the surface chemical composition on the blood compatibility of MSNs. They may cause hemolysis of red blood cells by deforming the cell membrane during particle endocytosis and thrombogenicity by activation of the blood coagulation cascade. Also, proteins can be non-specifically adsorbed to their surfaces, which may reduce the blood circulation time of nanoparticles.

(EDC) and *N*-hydroxysuccinimide (NHS) were purchased from Merck (Germany). 3-(Trihydroxysilyl)propyl methylphosphonate (TSPMP), human serum albumin (HSA), gamma globulins (γGs) from bovine serum, polyethylene glycol (PEG, M_w = 10 kDa), pyridine, ethanol, hydrochloric acid (37%) (HCl), and *n*-hexane were purchased from Sigma-Aldrich (USA). Mercaptopropyltrimethoxysilane (MPTMS), 3-(triethoxysilyl) propylisocyanate (TESPIC), and cetyltrimethylammoniumbromide (CTAB) were purchased from ABCR (Germany). DMSO was purchased from Carlo-Erba (Italy). All chemicals were used as purchased.

Synthesis of organosilane functionalized MSNs

All MSNs were synthesized by slightly modifying previous methods.[40–42] Briefly, 0.102 g of CTAB was dissolved in 50 mL of deionized water and 0.3 mL of 2 M NaOH was added. The reaction mixture was heated to 70 °C and 0.5 mL of TEOS was rapidly added under vigorous stirring (600 rpm). After 15 min, for A-MSN 80 μL of APTES, for P-MSN 180 μL of TSPMP (42 wt% in water), for M-MSN 49 μL of MTMS, for Ph-MSN 85 μL of PTES and for T-MSN 66 μL of MPTMS were added to satisfy the 0.15 organosilane/TEOS molar ratio. All organosilane monomers except TSPMP were first dissolved in 0.5 mL of ethanol and this solution was added dropwise. TSPMP was directly added. The reaction mixture was further stirred for 105 min. Also a non-functionalized MSN was prepared without the addition of any organosilane monomers. Finally, particles were collected by centrifugation at 8500 rpm for 15 min and washed with ethanol twice. To extract CTAB, MSNs were dispersed in 50 mL of 20 g L^{-1} ammonium nitrate solution in ethanol and stirred vigorously at 60 °C for 30 min. This treatment was repeated twice and the particles were washed with ethanol afterwards. The washed particles were added to 50 mL of 5 g L^{-1} HCl solution in ethanol and stirred vigorously at 60 °C for 30 min. Then, the particles were collected by centrifugation, washed with ethanol twice, and dispersed in 50 mL of ethanol.

Synthesis of Rhodamine B tagged MSN

To prepare R-MSN, 2 mg of RB dye was dissolved in 1 mL of DMSO and 9.3 μL of APTES was added. To this solution 3 mg of EDC and 2 mg of NHS were added and the reaction mixture was stirred at 200 rpm for 24 h at room temperature.[39] Then, the dye solution was added to the reaction mixture immediately after TEOS addition, whereas other reaction parameters were kept the same as with the MSN case.

Synthesis of PEGylated MSN

PEG (M_w = 10 kDa) was coupled with TESPIC through addition reaction between hydroxyl groups of PEG and isocyanate groups of TESPIC to prepare PEG-silane monomers.[36] Before the reaction, 100 mg of PEG was dried at 90 °C in a vacuum oven for 18 h. The dried PEG was dissolved in 30 mL of dry pyridine under an argon atmosphere by vigorous stirring at 70 °C for 6 h. Then, 2.63 mL of TESPIC was added to the reaction mixture and stirred for further 24 h. Pyridine was removed by rotary evaporation and a yellowish product was obtained. The raw product was washed twice with *n*-hexane. Then, the product was dissolved in ethanol at 35 °C (at room temperature the product is poorly soluble in ethanol) and precipitated at 4 °C overnight. Finally, the PEG-silane monomer precipitate was dissolved in 30 mL of ethanol and stored at 4 °C.

To graft the PEG-silane to the MSN surface, 20 mg of MSN was suspended in 24 mL of acidic (pH = 4) ethanol–water mixture (volume ratio, 1 : 2) and 1.5 mL of PEG-silane monomer solution was added to this solution under stirring at 600 rpm. After 24 h, the product was precipitated by centrifugation at 8500 rpm for 15 min and washed with water twice.

Hemolysis assay

Hemolysis experiments were performed according to previous reports.[19,20] EDTA stabilized human blood samples were freshly obtained from volunteers at Bilkent University Health Center (Ankara, Turkey). First, 3 mL of blood was centrifuged at 1600 rpm for 5 min and blood plasma and the surface layer were removed. The remaining RBC pellet was washed five times with 6 mL of PBS solution and RBCs were diluted in 25 mL of PBS solution. Then, 0.8 mL of MSN solutions in PBS at different concentrations were added to 0.2 mL of RBC suspension. Also, positive and negative control samples were prepared by adding 0.8 mL of water and PBS, respectively to 0.2 mL of RBC solution. Then, the samples were incubated at room temperature for 2 h. The samples were slightly shaken once for every 30 min to resuspend the RBCs and MSNs. After 2 h, the samples were centrifuged at 1600 rpm and 100 μL of supernatants was transferred to a 96-well plate. Absorbance of hemoglobin in supernatants was measured with a microplate reader at 570 nm. Also, the absorbance at 655 nm was recorded as the reference. Hemolysis percentages of the RBCs were calculated using the following formula:

$$\%\text{Hemolysis} = (\text{abs of sample} - \text{abs of negative control})/(\text{abs of positive control} - \text{abs of negative control})$$

Percent hemolysis values were calculated from three separate experiments. Student's *t*-test was applied to all datasets and the difference between them was accepted to be statistically significant when $p < 0.05$.

Coagulation assay

Samples for PT and aPTT were prepared according to a previous method.[43] Briefly, 40 μL of particles in PBS was mixed with 360 μL of freshly prepared plasma from citrated blood samples to give final particle concentrations of 0.1 or 1 mg mL^{-1}, and incubated for 5 min at 37 °C. Then the particles were centrifuged and 50 μL portions of supernatants were used to measure PT and aPTT values using a semi-automatic blood coagulation analyzer (Tokra Medikal, Ankara, Turkey). Control samples were prepared using 40 μL of PBS. All PT and aPTT values were calculated from at least three separate measurements.

Non-specific protein adsorption

Non-specific protein adsorption of MSNs was determined by mixing 0.5 mL of 0.6 mg mL^{-1} protein solution in phosphate

buffer with 0.5 mL of MSN solution in PBS at 2 mg mL^{-1} for HSA and 1 mg mL^{-1} for γGs.[36] All samples were shaken for 2 h at 37 °C and then particles were precipitated by centrifugation at 8500 rpm for 15 min. The absorbance of proteins in the supernatants at 280 nm was recorded using a UV-Vis spectrophotometer. The adsorbed protein percentages were calculated using a calibration curve. Protein adsorption percentages were calculated from three separate experiments.

Characterization

Transmission electron microscopy (TEM) images were taken using a Tecnai G2 F30 (FEI) microscope. X-ray powder diffraction (XRD) spectra were taken using an X'Pert Pro (Panalytical). Thermal gravimetric analyses (TGA) were performed with Q500 (TA Instruments). FTIR spectra of MSNs were collected by using a Fourier transform infrared spectrometer (FTIR, Vertex 70, Bruker). Zeta potentials of MSNs were measured with Zetasizer Nanoseries (Malvern Instruments). Optical absorption measurements of the released hemoglobin were carried out using a Microplate reader (Spectramax M5, Molecular Devices). Optical absorption measurements of proteins were carried out using a UV-Vis-NIR spectrophotometer (Cary 5000, Varian). The fluorescence spectrum of R-MSN was recorded with an Eclipse spectrophotometer (Varian).

Results

Synthesis and characterization of MSNs

Organosilane functionalized mesoporous silica nanoparticles were synthesized *via* sequential condensation of tetraethyl orthosilicate (TEOS) and organosilane monomers in the presence of the surfactant cetyltrimethylammoniumbromide (CTAB) under basic conditions.[40–42] Five different organosilane monomers were selected to obtain MSNs with diverse surface properties (Table 1). Positively charged aminopropyl, negatively charged methylphosphonate propyl, hydrophobic methyl and phenyl, and polar mercaptopropyl functionalized mesoporous silica nanoparticles were synthesized and named as A-MSN, P-MSN, M-MSN, Ph-MSN and T-MSN, respectively. All MSNs were synthesized using a 0.15 organosilane monomer/TEOS molar ratio and organosilane monomers were added 15 min after the TEOS addition to form organosilane rich surfaces.[41] Also, non-functionalized mesoporous silica nanoparticles (MSNs) were prepared without addition of any organosilane monomer. In addition, we prepared fluorescently tagged MSNs using Rhodamine B (RB) dye to evaluate the effect of fluorescent tagging on blood compatibility of MSNs. In order to attach the RB to the silica network, we first conjugated it with APTES in the presence of EDC/NHS. Then TEOS and the dye solution were polymerized in basic CTAB solution. All parameters were the same as with MSN synthesis except the addition of the RB-APTES conjugate.

PEGylated nanoparticles, as well as MSNs, have been studied by several groups and they were well-characterized in terms of hemolytic activity, thrombogenicity and non-specific protein adsorption.[35,36] Therefore, in this study we also prepared a PEGylated MSN (PEG-MSN) as the control. PEG-MSN was synthesized according to a previous report.[36] In brief, PEG (molecular weight = 10 kDa) was grafted to the MSN surface after conjugation with TESPIC.

Fig. 1a–d show the TEM images of MSNs (Fig. 1a and b) and P-MSNs (Fig. 1c and d). The particle size distributions were calculated based on TEM images and are given as insets in Fig. 1a and c. TEM images of other nanoparticles are given in the ESI (Fig. S1†) and the particle diameters of all MSNs are summarized in Table 1. All MSNs are spherical and they have similar particle sizes of around 80 nm with the exception of R-MSN; the average particle diameter of R-MSN is 62 ± 12 nm, and they are fairly monodisperse. Also, after PEGylation a thin organic layer is observed around the MSN from the TEM image of PEG-MSN (Fig. S2, ESI†) and the particle size is slightly increased to 80 nm from 78 nm (Table 1). The mesoporous structure of the particles can be clearly observed from the TEM images and pore sizes were found to be around 2–3 nm. The pore structure of the particles was further investigated by XRD (Fig. 1e). All particles exhibited characteristic diffraction peaks, (100), (110), and (200), of the highly ordered hexagonal pore structure of MCM-41 type mesoporous materials. The interplanar $d(100)$ spacing values of all MSNs are given in Table 1. The $d(100)$ values of particles are very close to each other (except for R-MSN which is slightly higher than others) indicating that functionalization with organosilane monomers did not

Table 1 Physical properties of mesoporous silica nanoparticles

Sample	Surface functionality	Method	Organosilane monomer[a] mol(%)	Size (TEM) (nm)	d_{100}[b] (nm)	TGA weight loss[c] (%)	Organic content[d] mol(%)
MSN	–OH	Co-condensation	0	78 ± 15	4.18	7.0	0
A-MSN	$-(CH_2)_3-NH_2$	Co-condensation	15	75 ± 14	4.18	15.4	8.7
P-MSN	$-(CH_2)_3-P(CH_3)O_3^-$	Co-condensation	15	81 ± 12	4.13	10.3	1.6
M-MSN	$-CH_3$	Co-condensation	15	76 ± 13	4.08	8.8	8.0
Ph-MSN	$-C_6H_5$	Co-condensation	15	83 ± 11	4.13	16.3	8.5
T-MSN	$-(CH_2)_3-SH$	Co-condensation	15	82 ± 15	4.06	15.4	7.8
R-MSN	$-(CH_2)_3-RB$	Co-condensation	n/a	62 ± 12	4.3	11.5	n/a
PEG-MSN	$-[OC_2H_4]_n-OH$	Grafting	n/a	80 ± 13	n/a	17.5	0.076

[a] Ratio to TEOS. [b] Interplanar spacing. [c] At 800 °C. [d] From TGA results.

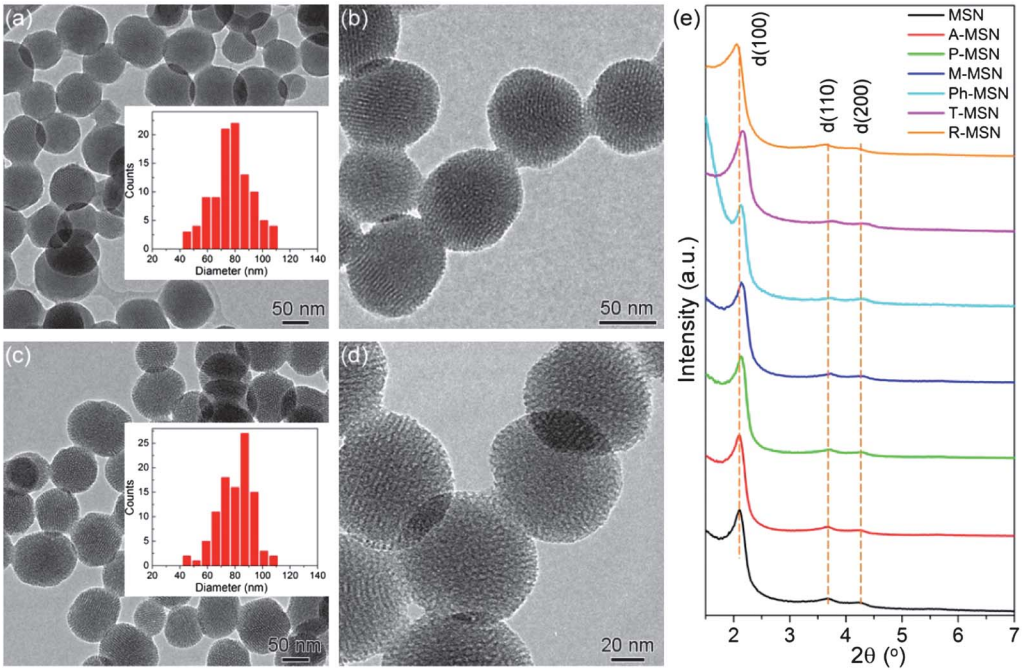

Fig. 1 TEM images of (a and b) MSNs and (c and d) P-MSNs. The uniform size distribution and mesoporous structure of the particles can be clearly observed from TEM images. The insets in (a and c) show the particle size distribution of MSNs and P-MSNs, respectively. The histograms were generated by measuring the diameter of 100 particles from the TEM images. (e) XRD spectra of all MSNs. For all particles characteristic peaks, *d*(100), *d*(110) and *d*(200), of the highly ordered hexagonal pore structure of MCM-41 type materials are clearly observable.

significantly affect the pore structure of MSNs. For R-MSN, the observed decrease in particle size and increase in *d*(100) spacing result from the interaction of bulky RB molecules with the CTAB micelles.[44] Nevertheless, R-MSN exhibits comparable particle size and pore structure with other particles.

Functionalization of MSNs with organosilane monomers was verified by TGA and FTIR. The TGA spectra of all particles are given in Fig. 2. The weight loss at 800 °C is between 8.8% and 16.3% for organosilane functionalized MSNs and 7% for bare MSN. The difference in weight loss between MSN and functionalized MSNs can be attributed to decomposable organosilane groups. Also, for PEG-MSN a large weight loss of 17.5% was observed. Based on TGA results, the molar organic content of functionalized MSNs was calculated and is given in Table 1. For R-MSN it is impossible to calculate the exact molar content of conjugated RB molecules because of the excess APTES monomer used during the synthesis, which can also bind to the silica network. Therefore, to further prove the successful RB conjugation we give the fluorescence spectrum of R-MSN (Fig. S3, ESI†), which demonstrates the bright fluorescence of R-MSN originated from RB dye. The organic contents of other particles are variable although they were synthesized under the same conditions. For all MSNs except P-MSN, highly functionalized MSNs (7.8 to 8.7 mol%) were obtained. On the other hand, for P-MSN the organic molar content is only 1.6%. The diversity of the organic content values can be attributed to the difference in the reactivity of organosilane monomers in synthesis solution. Also, for PEG-MSN 0.076 mol% grafting of PEG molecules to the MSN surface was calculated according to the TGA results. FTIR spectra of particles are given in the ESI (Fig. S4†). The –CH absorption peak at around 3000 cm^{-1} was observed for all functionalized particles indicating the presence of organic groups. Also, the same peak was observed in the bare MSN spectrum, which may be because of residual CTAB. Yet, the –CH absorption peak of bare MSNs was weaker than that of functionalized MSNs. Furthermore, some additional peaks were observed for functionalized MSNs. For example, for Ph-MSN the absorption peaks of the aromatic ring at 700 and 740 cm^{-1} and for PEG-MSN the absorption peaks of C–H bonds at 1350 and 1465 cm^{-1} are clearly observable.

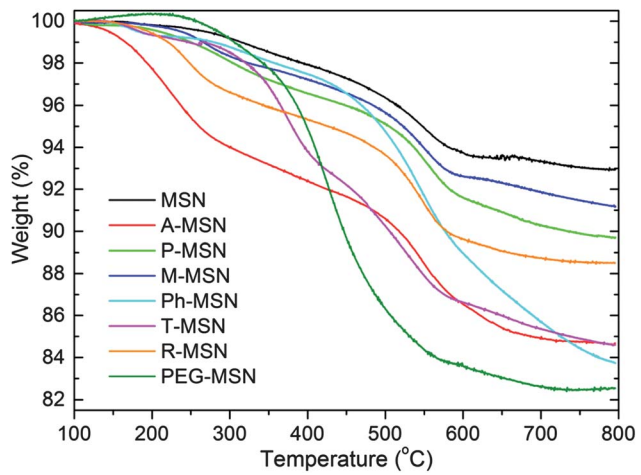

Fig. 2 Thermogravimetric analysis spectra of all MSNs. The weight loss for the MSNs which were functionalized with organosilane monomers is higher than bare MSNs because of decomposition of organic moieties at high temperatures.

Table 2 Zeta potentials of mesoporous silica nanoparticles

Sample	Zeta potential (mV) in PBS at pH 7.4
MSN	−22.4
A-MSN	0.6
P-MSN	−21.7
M-MSN	−15.9
Ph-MSN	−20.4
T-MSN	−21.3
R-MSN	−9.77
PEG-MSN	−18.9

The zeta potentials of MSNs in PBS solution were measured in order to characterize their surface properties (Table 2). The surface of bare MSNs is highly negative; the zeta potential is −22.4 mV, because of negatively charged silanol groups. Aminopropyl functionalized A-MSN exhibits a positive surface charge (0.6 mV). The positive zeta potential is because of the replacement of silanol groups with positively charged aminopropyl groups. Also, positively charged RB conjugation increased the zeta potential of MSN to −9.77 mV. Surface modification with negatively charged methylphosphonate does not significantly affect the zeta potential (−21.7 mV) of the MSNs due to having the same charge as silanol groups. Also, for particles with uncharged functional groups (M-MSN, Ph-MSN, T-MSN, and PEG-MSN) zeta potential becomes less negative due to the replacement of silanol groups with uncharged groups.

Hemolytic activity of MSNs

A hemolysis assay was used to determine the toxicity of MSNs on RBCs. 0.2 mL of isolated RBCs (see the Experimental section) was mixed with 0.8 mL of nanoparticles in PBS to give the desired MSN concentration, at a range of 0.05 to 1 mg mL^{-1}, and incubated at room temperature for 2 hours. Also, positive and negative control samples were prepared by adding 0.8 mL of water and PBS, respectively to RBCs. For every 30 min precipitated cells and particles were resuspended by gentle shaking. Hemolytic activity of MSNs was determined by measuring the absorption peak of hemoglobin at 570 nm, which was released to the solution from hemolyzed cells.[19,20]

Hemolysis results for all MSNs are given in Fig. 3. The highest hemolytic activity was observed for bare MSNs (5.5% at 0.1 mg mL^{-1} and 46.5% at 1 mg mL^{-1}). On the other hand, all MSNs functionalized with organic groups were demonstrated to have reduced or no hemolytic activity (Fig. 3a). Also, photographs showing precipitated RBCs at the end of the hemolysis experiment are given in Fig. 3b. The red color of the released hemoglobin from damaged cells is clearly observable for MSN, M-MSN, and Ph-MSN. For A-MSN, P-MSN, T-MSN, and PEG-MSN the supernatants are almost colorless at all concentrations. The functionalization of MSNs with charged or polar groups (A-MSN, P-MSN, T-MSN and R-MSN) can almost completely prevent the hemolytic activity. We observed 1.1%, 2.0% and 2.2% hemolysis for P-MSN, T-MSN and R-MSN, respectively at 1 mg mL^{-1} and for all other cases there were no detectable hemolysis for these three MSNs. Also, surface modification with PEG significantly reduced the hemolytic activity of MSNs (1.1% at 1 mg mL^{-1}) as previously reported.[36] Surface modifications with hydrophobic methyl and phenyl groups did not completely prevent the hemolytic activity but significantly reduced it. Ph-MSN did not exhibit any hemolytic activity up to 0.25 mg mL^{-1}; however, after that concentration the hemolysis percentage dramatically increased. M-MSN

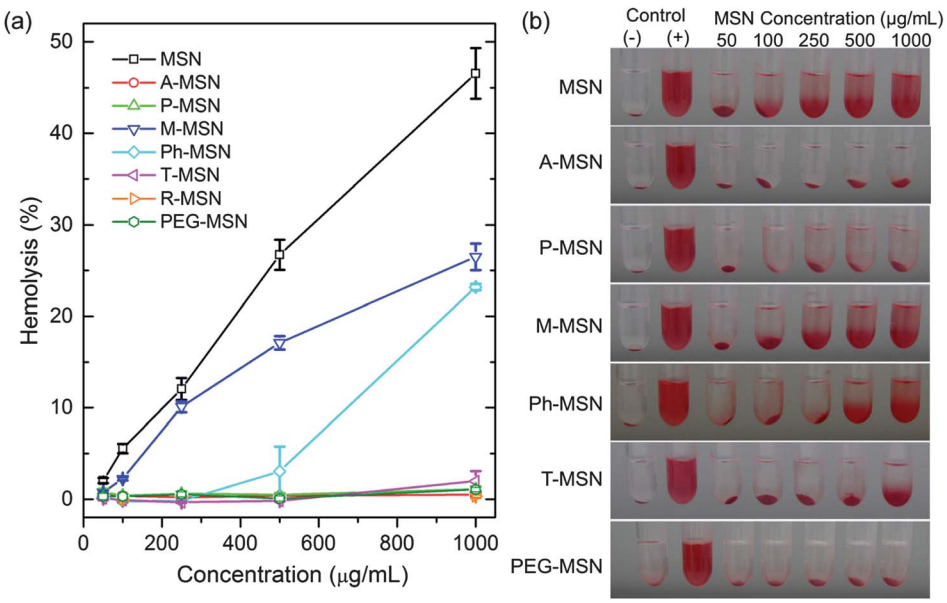

Fig. 3 Hemolysis results. (a) Hemolysis percentages of all MSNs at different concentrations between 0.05 and 1 g mL^{-1}, which were incubated with RBCs for 2 h. Data generated from three independent experiments. All functionalized MSNs demonstrated lower hemolytic activity compared to the bare MSN at all concentrations. Furthermore, for A-MSN, P-MSN, T-MSN, R-MSN and PEG-MSN almost no hemolytic activity was detected. (b) Photographs of RBCs treated with all MSNs at different concentrations. The released hemoglobin from the damaged cells in the supernatant can be seen from the photographs. (−) and (+) controls are the RBCs in PBS and water, respectively. Student's *t* test analyses revealed the statistical significance of the data ($p < 0.0001$).

exhibited hemolytic activity for all concentrations, yet it was lower than the hemolytic activity of MSNs for all cases.

It was reported that hemolysis assays may give false negative results because of adsorption of hemoglobin on particle surfaces[45] and false positive results because of the toxicity of the residual CTAB surfactant.[20] The adsorption of hemoglobin on particle surfaces can cause the removal of hemoglobin from the solution during centrifugation; therefore, lower hemolysis percentages than their actual values might be calculated. To investigate the adsorption of hemoglobin on MSN surfaces, we incubated MSN and A-MSN with the positive control sample (all RBCs are lysed with deionized water and all hemoglobin is released) for two hours (final particle concentration is 1 mg mL^{-1}) and the absorbance of hemoglobin at 570 nm was measured after precipitating MSNs with centrifugation. There is no significant difference between MSN and A-MSN treated and control samples. Thus, it can be said that only a small percentage of total proteins in the solution adsorbed on the surface of nanoparticles. The possible hemolysis due to toxicity of residual CTAB was investigated by treating the RBCs with the supernatant of 1 mg mL^{-1} MSN solution for two hours. The supernatant did not cause any hemolysis. Therefore, we verified that adsorption of hemoglobin by MSNs or effects of toxicity of residual CTAB do not interfere with the hemolysis assay used in this study.

We also examined the effect of surface functional group density on hemolysis by aminopropyl functionalized particles prepared using APTES to TEOS molar percentages between 2.5% and 15%. The MSNs were named as A_x-MSN, where x is the APTES to TEOS molar percentage. All aminopropyl functionalized MSNs are listed in Table 3. The organic contents of the MSNs were determined using the TGA method (Fig. S5, ESI†). The weight loss of MSNs gradually increases with increasing APTES amount as expected. Based on TGA results, organic contents of the A-MSNs were calculated and are given in Table 3. The zeta potentials of the particles are also given in Table 3. As the APTES ratio decreases the zeta potential of the particles becomes more negative because of reduction in the number of positively charged surface aminopropyl groups.

Hemolysis caused by aminopropyl modified MSNs at 0.1 and 1 mg mL^{-1} particle concentrations is given in Fig. 4. The hemolytic activity of the MSNs significantly reduced even at low amounts of (2.5%) aminopropyl functionalization. We observed 2.2% hemolysis only when the cells are incubated with $A_{2.5}$-MSNs at 1 mg mL^{-1}. At the same concentration bare MSN particles induced 46.5% hemolysis. For all other cases there was no detectable hemolysis for A-MSNs.

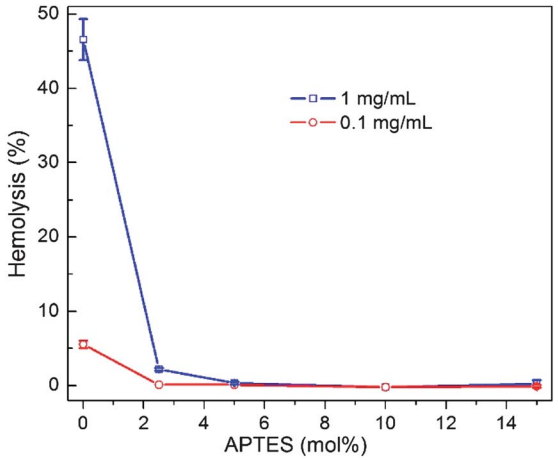

Fig. 4 Hemolytic activity of MSNs functionalized with APTES between 2.5 and 15 mol% with respect to TEOS. Even a small amount of APTES can dramatically decrease the hemolytic activity of MSNs. For the MSN functionalized using 2.5% APTES, 2.2% hemolysis was observed at 1 mg mL^{-1}. For all other APTES functionalized particles no hemolytic activity was detected at 1 mg mL^{-1}. At 0.1 mg mL^{-1} none of the particles resulted in hemolysis. Student's t test analyses revealed the statistical significance of the data ($p < 0.0001$).

Lastly, we showed that high hemolytic activity of the MSN can be reduced by interacting particles with human serum albumin (HSA) before the hemolysis experiment. 2.5 mg mL^{-1} of MSNs in PBS were incubated with different amounts of HSA for 1 h. The HSA concentration was varied between 0.01 mg mL^{-1} and 1 mg mL^{-1}. The hemolysis results of MSNs pre-interacted with HSA at 1 mg mL^{-1} particle concentration (Fig. S6, ESI†) revealed a gradual decrease in the hemolytic activity of MSNs with increasing HSA concentration. At 1 mg mL^{-1} HSA concentration we observed a hemolytic activity of only 1%.

Table 3 Organic contents and zeta potentials of aminopropyl functionalized MSNs

Sample	TGA weight loss[a] (%)	Organic content[b] mol(%)	Zeta potential (mV)
A_{15}-MSN	15.4	8.7	0.6
A_{10}-MSN	14.2	7.6	−3.1
A_5-MSN	13.1	6.4	−8.1
$A_{2.5}$-MSN	11.6	4.8	−10.5

[a] At 800 °C. [b] From TGA results.

Blood coagulation experiments

To study the thrombogenicity of the MSNs, we measured the PT and aPTT of nanoparticles at two different particle concentrations, 0.1 mg mL^{-1} and 1 mg mL^{-1}. PT is used to investigate extrinsic coagulation pathways and aPTT is used to investigate intrinsic coagulation pathways. Also, both methods are used to evaluate the common coagulation pathways.[43] Fig. 5 shows the PT and aPTT results of MSNs. The PT and aPTT results revealed that none of the functionalized or bare particles result in a significant activation of common, intrinsic or extrinsic pathways of coagulation.

Administration of MSNs to the blood serum slightly reduced the PT compared to the control at both concentrations; however all values were within the expected range (*i.e.* the ratio between PT values of MSN treated serum and control serum is between 0.82 and 1.15). Also, we did not observe any alteration in the aPTT of MSNs at 0.1 mg mL^{-1}. All aPTT values were in their normal range, which is between 25 and 36 s. However, at 1 mg mL^{-1} we observed significantly prolonged coagulation times for MSN, P-MSN, R-MSN and PEG-MSN. In addition, aPTT of P-MSN

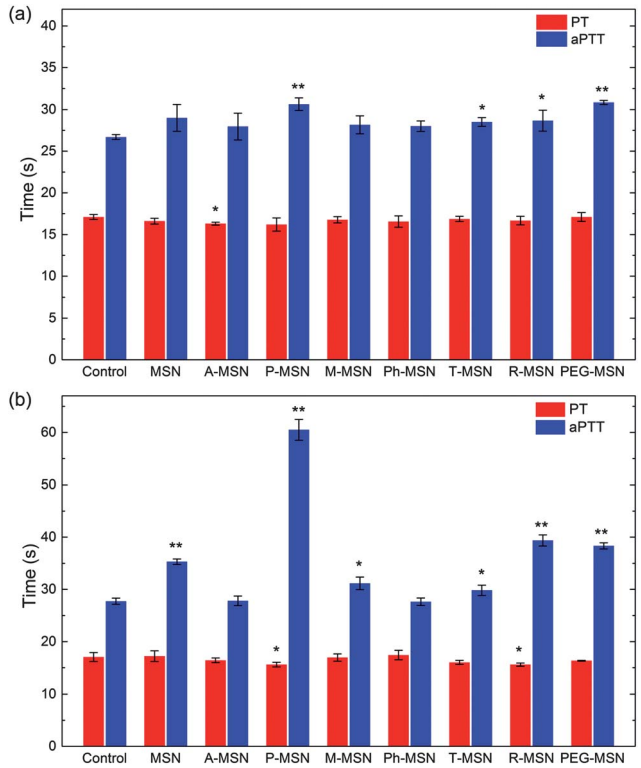

Fig. 5 PT and aPTT measurements of particles. (a) 0.1 mg mL^{-1} particle concentration. All PT and aPTT values are within their normal range. (b) 1 mg mL^{-1} particle concentration. All PT values are within their normal range; however, aPTT values for R-MSN and especially for P-MSN are higher than the normal value, which indicates that these particles inhibit the intrinsic pathways of coagulation at this concentration. Data were generated from at least three independent experiments. According to Student's *t* test, $*p < 0.05$ and $**p < 0.0001$.

is significantly higher than the upper limit of the normal values, which is 60.5 ± 2 s. In other words, P-MSN showed moderate anticoagulation behavior at 1 mg mL^{-1} concentration by inhibiting the intrinsic pathways of coagulation.[46]

Non-specific protein adsorption

We studied non-specific protein adsorption on surfaces of MSNs using HSA and γGs which are the most abundant proteins in human blood (HSA is 60% and Gs is 18% of the total serum proteins).[36] Also, adsorption of γGs to nanoparticle surfaces is particularly important because these proteins can mark the foreign particles and make them visible to the mononuclear phagocyte system (opsonization), which leads to rapid clearance of nanoparticles from blood.[47] Particles in PBS were mixed with protein solution in phosphate buffer (pH 7.4) to give a final concentration of 0.3 mg mL^{-1} proteins. The solutions were shaken at 37 °C for 2 hours and the nanoparticles were precipitated by centrifugation. The percentage of adsorbed proteins on MSNs was calculated by monitoring the absorption band of proteins at 280 nm before and after interacting with MSNs.

Fig. 6 shows the amount of adsorbed proteins on nanoparticle surfaces compared to MSNs. Also, adsorbed protein amounts are listed in Table 4. PEGylation significantly reduced the non-specific protein adsorption to the MSN surface, as

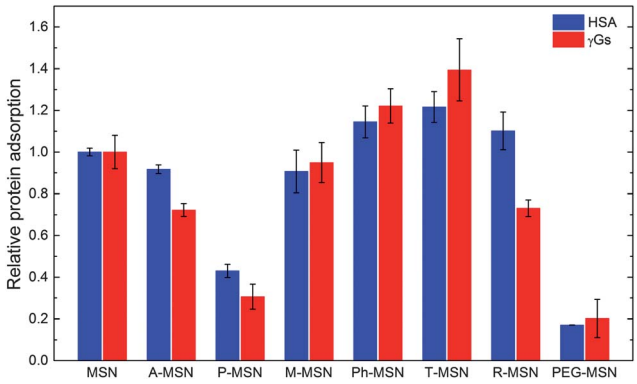

Fig. 6 Protein adsorption percentages of nanoparticles. Data were generated from three independent experiments.

Table 4 Protein adsorption amounts of MSNs

	Adsorbed protein (nmol mg^{-1} MSN)	
Sample	HSA	γGs
MSN	6.98 ± 0.12	1.28 ± 0.1
A-MSN	6.4 ± 0.14	0.92 ± 0.04
P-MSN	3.0 ± 0.2	0.39 ± 0.08
M-MSN	6.32 ± 0.66	1.22 ± 0.12
Ph-MSN	8.0 ± 0.5	1.56 ± 0.1
T-MSN	8.5 ± 0.48	1.78 ± 0.18
R-MSN	7.7 ± 0.58	0.94 ± 0.05
PEG-MSN	1.2 ± 0.004	0.26 ± 0.12

previously reported.[36] Interestingly, protein adsorption of A-MSN and especially P-MSN is significantly lower than MSN for both HSA and γGs. Modification of the MSN surface with small methyl groups did not significantly affect the protein adsorption properties. On the other hand, phenyl and mercaptopropyl modification largely increases the adsorption of HSA and γGs to the MSN surfaces. Lastly, positively charged and hydrophobic RB modification resulted in a slight increase in HSA adsorption but significant decrease in γGs adsorption.

Discussion

Blood compatibility is probably the most critical issue regarding administration of MSNs as drug or biomolecule carriers and theranostic agents, not only because their interactions with blood constituents in the circulatory system can result in significant toxicity to organisms, but also cell membrane–nanoparticle interactions are quite similar for all cell types. Surface composition of MSNs is one of the predominant factors determining these interactions, the fundamentals of which have not been elaborately comprehended yet. In this context, we systematically studied blood compatibility of mesoporous silica nanoparticles possessing ionic, hydrophobic or polar surface functional groups, in terms of their hemolytic activity, thrombogenicity and non-specific protein adsorption.

There are some reports[16,19,36] that investigate surface effects on interactions of MSNs with biological systems in terms of

cellular uptake, cytotoxicity, hemolytic activity and non-specific protein adsorption. However, previous reports generally categorized the surfaces simply as positive (aminopropyl modified), negative (bare) and neutral (PEGylated). On the other hand, our research demonstrates that interactions between the MSN surface and biological systems are much more complicated than that and cannot be evaluated on the basis of only surface charge. For instance, bare MSN and P-MSN both demonstrate highly negative surface charge, but their hemolytic activity, thrombogenicity and non-specific protein adsorption properties are all completely different.

Recently, Slowing *et al.*[18] observed that hemolytic activity of MSNs can be prevented by modifying the surface with some ionic surface functional groups, such as aminopropyl and carboxylic acid. In contrast, Yu *et al.*[22] reported that aminopropyl modification increases the hemolytic activity of silica nanoparticles. Also, there is a disagreement in the origin of the hemolytic activity of silica nanoparticles. Slowing *et al.*[18] claimed that the hemolytic activity of silica nanoparticles is related to the surface silanol groups; on the other hand, Yu *et al.*[22] concluded that it is related to the zeta potential of the surface. Therefore, to clarify these points and understand the surface effects on hemolytic activity elaborately, in this study we used a large library of surface functional groups with different characteristics (*i.e.* hydrophobic, aromatic, polar, neutral, positively charged and negatively charged). Our results (Fig. 3) indicate that there is no correlation between the net surface charge (zeta potential) and hemolytic activity of MSNs (in the studied zeta potential range, between −22 and 1 mV); instead it is very specific to the number of accessible surface silanol groups regarding the RBC membrane. We observed that the hemolytic activity of MSNs can be prevented almost completely in the studied concentration range by modifying the MSN surfaces with bulky—compared to other functional groups—aminopropyl, methylphosphonate propyl, mercaptopropyl, RB and PEG moieties. The improved compatibility of these MSNs with RBCs mainly results from the reduced number of accessible surface silanol groups by steric hindrance of the bulky functional groups. Also, A-MSN, T-MSN, R-MSN and PEG-MSN are not expected to electrostatically interact with positively charged trimethyl-ammonium head groups of the cell membrane lipids since their functional groups are positively charged or neutral at pH 7.4.[48] In addition, we observed that even a small amount of positively charged and bulky aminopropyl functionalization can dramatically reduce the hemolytic activity of MSNs (Fig. 4) by preventing the interaction of silanol groups with cell membranes. Furthermore, the silanol specificity of hemolytic activity of silica particles was also shown by coating the particles with HSA. The HSA corona formed around the particles blocks the surface silanol groups and results in a significant decrease in the hemolytic activity.[49]

Interestingly, the negatively charged P-MSN (zeta potential is −21.7 mV, which is very close to that of bare MSN) also did not cause significant hemolysis although electrostatic interaction between methylphosphonate and the positively charged RBC membrane could be expected. The energy released from the binding of the MSN to the RBC membrane and the free energy required for bending of the RBC membrane around MSNs are two competitive parameters that determine the interaction among MSNs and RBCs. If the energy released through binding is greater than the energy required for bending, endocytosis of MSNs occurs.[19,48,50,51] The released energy during binding of P-MSN to the RBC membrane is expected to be less than the released energy during MSN binding, because methylphosphonate is a softer ligand than silanol, which may not meet the energy requirement for excessive membrane bending needed for endocytosis of particles. It can be concluded that P-MSN did not cause any significant hemolysis because of its low binding affinity to the RBC membrane.

Also, small methyl and phenyl functional groups can decrease the hemolytic activity of MSNs to a degree. One reason for lower hemolytic activity of these particles relative to the bare MSNs may be the replacement of some surface silanol groups with methyl and phenyl groups. In addition, methyl and phenyl groups can also hinder the interaction among silanol groups and the RBC membrane; however, they might not be bulky enough to prevent the interaction completely.

It has been reported that dry mesoporous silica materials can be used to increase the rate of hemostasis by activating coagulation pathways due to their high absorption capacities.[29] However, PT and aPTT results revealed that MSNs prepared in this work did not activate extrinsic, intrinsic or common coagulation pathways up to a concentration of 1 mg mL^{-1}. This guarantees that particles do not have any thrombogenic activity in the studied concentration range. The observed low coagulant behavior of MSNs can be explained by the already PBS filled pores of these materials, which significantly diminish the absorption capacity of particles compared to their dry state.[35,43] Also, it should be noted that the highest concentration used for thrombogenicity experiments in this study, 1 mg mL^{-1}, was roughly equal to a particle dose of 100 mg kg^{-1},[24] which is a sufficient dose for intravenous applications of MSNs.[52]

Surprisingly, we observed significantly prolonged aPTT values for P-MSN at 1 mg mL^{-1}, which indicate that P-MSN can inhibit the intrinsic coagulation pathways, but it does not have any significant effect on extrinsic coagulation pathways. Mechanisms causing the anticoagulant behavior of P-MSN are beyond the scope of this study, but definitely further experiments are required.

As in hemolytic activity experiments, there is no correlation between the surface charge of particles and their thrombogenicity. Negatively charged P-MSN showed significant anticoagulant behavior at 1 mg mL^{-1} concentration; however bare MSN did not show any anticoagulant behavior. Also, P-MSN and R-MSN were modified with negatively and positively charged functional groups, respectively, but both showed prolonged aPTT.

Protein surfaces are heterogeneous and contain charged, polar and hydrophobic moieties. Due to their various surface groups they can easily adsorb onto the surfaces *via* many interactions such as ionic and hydrophobic interactions and hydrogen bonding. Consequently, when nanoparticles are injected into the blood their surface is rapidly covered with a layer of blood proteins called protein corona.[33,53–55] For many biological applications, the non-specific protein adsorption on

the nanoparticle surfaces is undesirable because it increases the uptake of nanoparticles by immune cells, which reduce the blood circulation times. For effective use of nanoparticles in biological applications non-specific protein adsorption must be prevented or reduced to an appropriate level.[31]

We observed significantly lower protein adsorption for A-MSN, P-MSN and PEG-MSN than bare MSN. Although ionic aminopropyl and methylphosphonate propyl groups are expected to interact with proteins mainly through hydrogen bonding and ionic interactions, as silanol groups of MSN, the lower protein adsorption of A-MSN and P-MSN may arise from the steric repulsion of flexible propyl chains of their functional groups.[36] For M-MSN there is no statistically significant difference from MSN in adsorbed protein amounts which is because the methyl groups are not large enough to prevent interaction of silanol groups with proteins. On the other hand phenyl and mercaptopropyl modifications largely increase the protein adsorption for both HSA and γGs. The higher adsorption capacity of Ph-MSN and T-MSN can be attributed to their more complex surface structures, which can provide additional interactions, such as hydrophobic and polar interactions, for protein binding. For R-MSN, increased HSA adsorption and reduced γGs adsorption compared to MSN were observed. The high HSA adsorption of R-MSN can be attributed to its higher surface area than other particles due to its smaller particle size. However, R-MSN still adsorbs less γGs compared to MSNs.

PEGylated surfaces are for long known as protein resistant due to their hydrophilic and flexible nature.[56] Accordingly, Wang *et al.*[3] and He *et al.*[36] showed that adsorption of proteins on the MSN surface can be significantly reduced by grafting their surfaces with PEGylated coatings. Similarly, in this work 83% reduction in γGs and 80% reduction in HSA adsorption was observed for PEG-MSN. Surprisingly, here we observed comparable results (70% decrease for γGs and 57% decrease for HSA) that can be achieved by modifying the MSN surface with a small organosilane ligand, methylphosphonate propyl, using a facile one-pot method.

Conclusions

In this work, we studied the surface effects on blood compatibility of MSNs in terms of their hemolytic activity, thrombogenicity and non-specific protein adsorption. Bare MSNs were found to be very toxic to RBCs and caused significant hemolysis between 0.05 and 1 mg mL^{-1} concentrations. We observed that functionalization of MSNs with organosilane monomers significantly reduced or completely prevented the hemolytic activity of MSNs. Our observations show that the hemolytic activity of MSNs is very specific to the number of accessible surface silanol groups. PT and aPTT values of MSNs demonstrated that none of the particles activate the coagulation cascade in the studied concentration range. Also, we observed inhibition of intrinsic coagulation pathways in the presence of P-MSN at 1 mg mL^{-1}. Non-specific protein adsorption on the MSNs was tested by using HSA and γGs. We showed that protein adsorption on the MSN surface can significantly be reduced using aminopropyl and methylphosphonate propyl functional groups. In conclusion, this work demonstrated that blood compatibility of MSNs can be comprehended and improved in terms of surface functional groups. Also our results showed that interactions between MSNs and blood constituents are not simply dependent on the surface charge of particles; instead they are quite specific to the chemical composition of the surface functional groups. Certainly, more studies (*e.g.* cellular uptake and *in vivo* studies) are needed to fully understand the interactions between mesoporous silica drug carriers and biological systems. Nevertheless, we believe that our results provide researchers an adequate ground for hypothesizing blood compatibility of the MSNs according to the chemical composition of MSN surfaces.

Acknowledgements

We gratefully thank Prof. Adil Denizli, Nilay Bereli and Gülsu Şener for their help in coagulation experiments. This work was partially supported by Ministry of Development and TUBITAK under project no. 110M412 and 111T696. M.B. acknowledges partial support from the Turkish Academy of Sciences (TUBA).

References

1 Q. J. He and J. L. Shi, Mesoporous silica nanoparticle based nano drug delivery systems: synthesis, controlled drug release and delivery, pharmacokinetics and biocompatibility, *J. Mater. Chem.*, 2011, **21**, 5845–5855.
2 J. Lu, M. Liong, J. I. Zink and F. Tamanoi, Mesoporous silica nanoparticles as a delivery system for hydrophobic anticancer drugs, *Small*, 2007, **3**, 1341–1346.
3 L. S. Wang, C. L. Wu, S. Y. Lu, L. L. Chang, I. T. Teng, C. M. Yang and J. A. Ho, Biofunctionalized phospholipid-capped mesoporous silica nanoshuttles for targeted drug delivery: improved water suspensibility and decreased nonspecific protein binding, *ACS Nano*, 2010, **4**, 4371–4379.
4 C. Y. Liu, J. Guo, W. L. Yang, J. H. Hu, C. C. Wang and S. K. Fu, Magnetic mesoporous silica microspheres with thermo-sensitive polymer shell for controlled drug release, *J. Mater. Chem.*, 2009, **19**, 4764–4770.
5 M. H. Kim, H. K. Na, Y. K. Kim, S. R. Ryoo, H. S. Cho, K. E. Lee, H. Jeon, R. Ryoo and D. H. Min, Facile synthesis of monodispersed mesoporous silica nanoparticles with ultralarge pores and their application in gene delivery, *ACS Nano*, 2011, **5**, 3568–3576.
6 M. Liong, J. Lu, M. Kovochich, T. Xia, S. G. Ruehm, A. E. Nel, F. Tamanoi and J. I. Zink, Multifunctional inorganic nanoparticles for imaging, targeting, and drug delivery, *ACS Nano*, 2008, **2**, 889–896.
7 Y. S. Lin, C. P. Tsai, H. Y. Huang, C. T. Kuo, Y. Hung, D. M. Huang, Y. C. Chen and C. Y. Mou, Well-ordered mesoporous silica nanoparticles as cell markers, *Chem. Mater.*, 2005, **17**, 4570–4573.
8 J. E. Lee, D. J. Lee, N. Lee, B. H. Kim, S. H. Choi and T. Hyeon, Multifunctional mesoporous silica nanocomposite nanoparticles for pH controlled drug release and dual modal imaging, *J. Mater. Chem.*, 2011, **21**, 16869–16872.

9 A. M. Sauer, A. Schlossbauer, N. Ruthardt, V. Cauda, T. Bein and C. Brauchle, Role of endosomal escape for disulfide-based drug delivery from colloidal mesoporous silica evaluated by live-cell imaging, *Nano Lett.*, 2010, **10**, 3684–3691.

10 J. E. Lee, N. Lee, T. Kim, J. Kim and T. Hyeon, Multifunctional mesoporous silica nanocomposite nanoparticles for theranostic applications, *Acc. Chem. Res.*, 2011, **44**, 893–902.

11 S. H. Cheng, C. H. Lee, M. C. Chen, J. S. Souris, F. G. Tseng, C. S. Yang, C. Y. Mou, C. T. Chen and L. W. Lo, Tri-functionalization of mesoporous silica nanoparticles for comprehensive cancer theranostics the trio of imaging, targeting and therapy, *J. Mater. Chem.*, 2010, **20**, 6149–6157.

12 X. Wang, H. Chen, Y. Chen, M. Ma, K. Zhang, F. Li, Y. Zheng, D. Zeng, Q. Wang and J. Shi, Perfluorohexane-encapsulated mesoporous silica nanocapsules as enhancement agents for highly efficient high intensity focused ultrasound (HIFU), *Adv. Mater.*, 2012, **24**, 785–791.

13 F. Wang, X. Chen, Z. Zhao, S. Tang, X. Huang, C. Lin, C. Cai and N. Zheng, Synthesis of magnetic, fluorescent and mesoporous core–shell-structured nanoparticles for imaging, targeting and photodynamic therapy, *J. Mater. Chem.*, 2011, **21**, 11244–11252.

14 M. Al-Shamsi, M. T. Al-Samri, S. Al-Salam, W. Conca, S. Shaban, S. Benedict, S. Tariq, A. V. Biradar, H. S. Penefsky, T. Asefa and A. K. Souid, Biocompatibility of calcined mesoporous silica particles with cellular bioenergetics in murine tissues, *Chem. Res. Toxicol.*, 2010, **23**, 1796–1805.

15 Q. He, Z. Zhang, Y. Gao, J. Shi and Y. Li, Intracellular localization and cytotoxicity of spherical mesoporous silica nano and microparticles, *Small*, 2009, **5**, 2722–2729.

16 Z. Tao, B. B. Toms, J. Goodisman and T. Asefa, Mesoporosity and functional group dependent endocytosis and cytotoxicity of silica nanomaterials, *Chem. Res. Toxicol.*, 2009, **22**, 1869–1880.

17 M. A. Maurer-Jones, Y. S. Lin and C. L. Haynes, Functional assessment of metal oxide nanoparticle toxicity in immune cells, *ACS Nano*, 2010, **4**, 3363–3373.

18 I. I. Slowing, C. W. Wu, J. L. Vivero-Escoto and V. S. Lin, Mesoporous silica nanoparticles for reducing hemolytic activity towards mammalian red blood cells, *Small*, 2009, **5**, 57–62.

19 Y. Zhao, X. Sun, G. Zhang, B. G. Trewyn, I. I. Slowing and V. S. Lin, Interaction of mesoporous silica nanoparticles with human red blood cell membranes: size and surface effects, *ACS Nano*, 2011, **5**, 1366–1375.

20 Y. S. Lin and C. L. Haynes, Impacts of mesoporous silica nanoparticle size, pore ordering, and pore integrity on hemolytic activity, *J. Am. Chem. Soc.*, 2010, **132**, 4834–4842.

21 L. C. Thomassen, V. Rabolli, K. Masschaele, G. Alberto, M. Tomatis, M. Ghiazza, F. Turci, E. Breynaert, G. Martra, C. E. Kirschhock, J. A. Martens, D. Lison and B. Fubini, Model system to study the influence of aggregation on the hemolytic potential of silica nanoparticles, *Chem. Res. Toxicol.*, 2011, **24**, 1869–1875.

22 T. Yu, A. Malugin and H. Ghandehari, Impact of silica nanoparticle design on cellular toxicity and hemolytic activity, *ACS Nano*, 2011, **5**, 5717–5728.

23 S. P. Hudson, R. F. Padera, R. Langer and D. S. Kohane, The biocompatibility of mesoporous silicates, *Biomaterials*, 2008, **29**, 4045–4055.

24 T. Yu, K. Greish, A. Malugin, L. D. McGill, A. Ray and H. Ghandehari, Influence of geometry, porosity, and surface characteristics of silica nanoparticles on acute toxicity: their vasculature effect and tolerance threshold, *ACS Nano*, 2012, **6**, 2289–2301.

25 K. Yamashita, Y. Yoshioka, K. Higashisaka, K. Mimura, Y. Morishita, M. Nozaki, T. Yoshida, T. Ogura, H. Nabeshi, K. Nagano, *et al.*, Silica and titanium dioxide nanoparticles cause pregnancy complications in mice, *Nat. Nanotechnol.*, 2011, **6**, 321–328.

26 S. Sharifi, S. Behzadi, S. Laurent, M. L. Forrest, P. Stroeve and M. Mahmoudi, Toxicity of nanomaterials, *Chem. Soc. Rev.*, 2012, **41**, 2323–2343.

27 H. B. Alam, Z. Chen, A. Jaskille, R. I. L. C. Querol, E. Koustova, R. Inocencio, R. Conran, A. Seufert, N. Ariaban, K. Toruno and P. Rhee, Application of a zeolite hemostatic agent achieves 100% survival in a lethal model of complex groin injury in swine, *J. Trauma*, 2004, **56**, 974–983.

28 T. A. Ostomel, Q. Shi and G. D. Stucky, Oxide hemostatic activity, *J. Am. Chem. Soc.*, 2006, **128**, 8384–8385.

29 C. L. Dai, Y. Yuan, C. S. Liu, J. Wei, H. Hong, X. S. Li and X. H. Pan, Degradable, antibacterial silver exchanged mesoporous silica spheres for hemorrhage control, *Biomaterials*, 2009, **30**, 5364–5375.

30 M. A. Dobrovolskaia, P. Aggarwal, J. B. Hall and S. E. McNeil, Preclinical studies to understand nanoparticle interaction with the immune system and its potential effects on nanoparticle biodistribution, *Mol. Pharmaceutics*, 2008, **5**, 487–495.

31 M. Cavadas, A. Gonzalez-Fernandez and R. Franco, Pathogen-mimetic stealth nanocarriers for drug delivery: a future possibility, *Nanomedicine*, 2011, **7**, 730–743.

32 J. M. Koziara, J. J. Oh, W. S. Akers, S. P. Ferraris and R. J. Mumper, Blood compatibility of cetyl alcohol/polysorbate-based nanoparticles, *Pharm. Res.*, 2005, **22**, 1821–1828.

33 P. Aggarwal, J. B. Hall, C. B. McLeland, M. A. Dobrovolskaia and S. E. McNeil, Nanoparticle interaction with plasma proteins as it relates to particle biodistribution, biocompatibility and therapeutic efficacy, *Adv. Drug Delivery Rev.*, 2009, **61**, 428–437.

34 D. E. Owens III and N. A. Peppas, Opsonization, biodistribution, and pharmacokinetics of polymeric nanoparticles, *Int. J. Pharm.*, 2006, **307**, 93–102.

35 H. Wu, S. Zhang, J. Zhang, G. Liu, J. Shi, L. Zhang, X. Cui, M. Ruan, Q. He and W. Bu, A hollow-core, magnetic, and mesoporous double-shell nanostructure: *in situ* decomposition/reduction synthesis, bioimaging, and drug-delivery properties, *Adv. Funct. Mater.*, 2011, **21**, 1850–1862.

36 Q. He, J. Zhang, J. Shi, Z. Zhu, L. Zhang, W. Bu, L. Guo and Y. Chen, The effect of PEGylation of mesoporous silica nanoparticles on nonspecific binding of serum proteins and cellular responses, *Biomaterials*, 2010, **31**, 1085–1092.

37 F. Lu, S. H. Wu, Y. Hung and C. Y. Mou, Size effect on cell uptake in well-suspended, uniform mesoporous silica nanoparticles, *Small*, 2009, **5**, 1408–1413.

38 B. Chang, J. Guo, C. Liu, J. Qian and W. Yang, Surface functionalization of magnetic mesoporous silica nanoparticles for controlled drug release, *J. Mater. Chem.*, 2010, **20**, 9941–9947.

39 Q. He, J. Shi, X. Cui, J. Zhao, Y. Chen and J. Zhou, Rhodamine B-co-condensed spherical SBA-15 nanoparticles: facile co-condensation synthesis and excellent fluorescence features, *J. Mater. Chem.*, 2009, **19**, 3395–3403.

40 Q. Cai, Z. S. Luo, W. Q. Pang, Y. W. Fan, X. H. Chen and F. Z. Cui, Dilute solution routes to various controllable morphologies of MCM-41 silica with a basic medium, *Chem. Mater.*, 2001, **13**, 258–263.

41 V. Cauda, A. Schlossbauer, J. Kecht, A. Zurner and T. Bein, Multiple core–shell functionalized colloidal mesoporous silica nanoparticles, *J. Am. Chem. Soc.*, 2009, **131**, 11361–11370.

42 A. Yildirim, H. Budunoglu, B. Daglar, H. Deniz and M. Bayindir, One-pot preparation of fluorinated mesoporous silica nanoparticles for liquid marble formation and superhydrophobic surfaces, *ACS Appl. Mater. Interfaces*, 2011, **3**, 1804–1808.

43 Q. He, J. Zhang, F. Chen, L. Guo, Z. Zhu and J. Shi, An anti-ROS/hepatic fibrosis drug delivery system based on salvianolic acid B loaded mesoporous silica nanoparticles, *Biomaterials*, 2010, **31**, 7785–7796.

44 C. Boissiere, M. A. U. Martines, M. Tokumoto, A. Larbot and E. Prouzet, Mechanisms of pore size control in MSU-X mesoporous silica, *Chem. Mater.*, 2003, **15**, 509–515.

45 M. A. Dobrovolskaia, J. D. Clogston, B. W. Neun, J. B. Hall, A. K. Patri and S. E. McNeil, Method for analysis of nanoparticle hemolytic properties *in vitro*, *NanoLett.*, 2008, **8**, 2180–2187.

46 F. Tong, X. Chen, L. Chen, P. Zhu, J. Luan, C. Mao, J. Bao and J. Shen, Preparation, blood compatibility and anticoagulant effect of heparin-loaded polyurethane microspheres, *J. Mater. Chem. B*, 2013, **1**, 447–453.

47 T. Ishida, H. Harashima and H. Kiwada, Interactions of liposomes with cells *in vitro* and *in vivo*: opsonins and receptors, *Curr. Drug Metab.*, 2001, **2**, 397–409.

48 Y. Roiter, M. Ornatska, A. R. Rammohan, J. Balakrishnan, D. R. Heine and S. Minko, Interaction of nanoparticles with lipid membrane, *Nano Lett.*, 2008, **8**, 941–944.

49 J. Shia, Y. Hedberg, M. Lundin, I. O. Wallinder, H. L. Karlsson and L. Möller, Hemolytic properties of synthetic nano and porous silica particles: the effect of surface properties and the protection by the plasma corona, *Acta Biomater.*, 2012, **8**, 3478–3490.

50 M. Deserno and W. M. Gelbart, Adhesion and wrapping in colloid–vesicle complexes, *J. Phys. Chem. B*, 2002, **106**, 5543–5552.

51 R. Lipowsky and H. G. Dobereiner, Vesicles in contact with nanoparticles and colloids, *Europhys. Lett.*, 1998, **43**, 219–225.

52 X. X. He, H. L. Nie, K. M. Wang, W. H. Tan, X. Wu and P. F. Zhang, *In vivo* study of biodistribution and urinary excretion of surface-modified silica nanoparticles, *Anal. Chem.*, 2008, **80**, 9597–9603.

53 T. Cedervall, I. Lynch, S. Lindman, T. Berggard, E. Thulin, H. Nilsson, K. A. Dawson and S. Linse, Understanding the nanoparticle protein corona using methods to quantify exchange rates and affinities of proteins for nanoparticles, *Proc. Natl. Acad. Sci. U. S. A.*, 2007, **104**, 2050–2055.

54 M. Lundqvist, J. Stigler, T. Cedervall, T. Berggrad, M. B. Flanagan, I. Lynch, G. Elia and K. Dawson, The evolution of the protein corona around nanoparticles: a test study, *ACS Nano*, 2011, **5**, 7503–7509.

55 E. Casals, T. Pfaller, A. Duschl, G. J. Oostingh and V. Puntes, Time evolution of the nanoparticle protein corona, *ACS Nano*, 2010, **4**, 3623–3632.

56 S. I. Jeon, J. H. Lee, J. D. Andrade and P. G. De Gennes, Protein-surface interactions in the presence of polyethylene oxide I. Simplified theory, *J. Colloid Interface Sci.*, 1991, **142**, 149–158.

Supplementary Information

Impact of mesoporous silica nanoparticle surface functionality on hemolytic activity, thrombogenicity and non-specific protein adsorption

Adem Yildirim [ab], Erol Ozgur [ab], Mehmet Bayindir [abc*]

[a]UNAM-National Nanotechnology Research Center, Bilkent University, 06800 Ankara, Turkey.

[b]Institute of Materials Science and Nanotechnology, Bilkent University, 06800 Ankara, Turkey

[c]Department of Physics, Bilkent University, 06800 Ankara, Turkey

[*]Corresponding author: *E-mail: bayindir@nano.org.tr*

We have provided TEM images of A-MSN, M-MSN, Ph-MSN, T-MSN, R-MSN and PEG-MSN (Fig. S1 and S2); Fluorescence spectrum of R-MSN (Fig. S3); FTIR spectra of all eight MSNs (Fig. S4); TGA spectra of aminopropyl functionalized MSNs (Fig. S5); and Hemolysis results of HSA coated MSNs (Fig. S6).

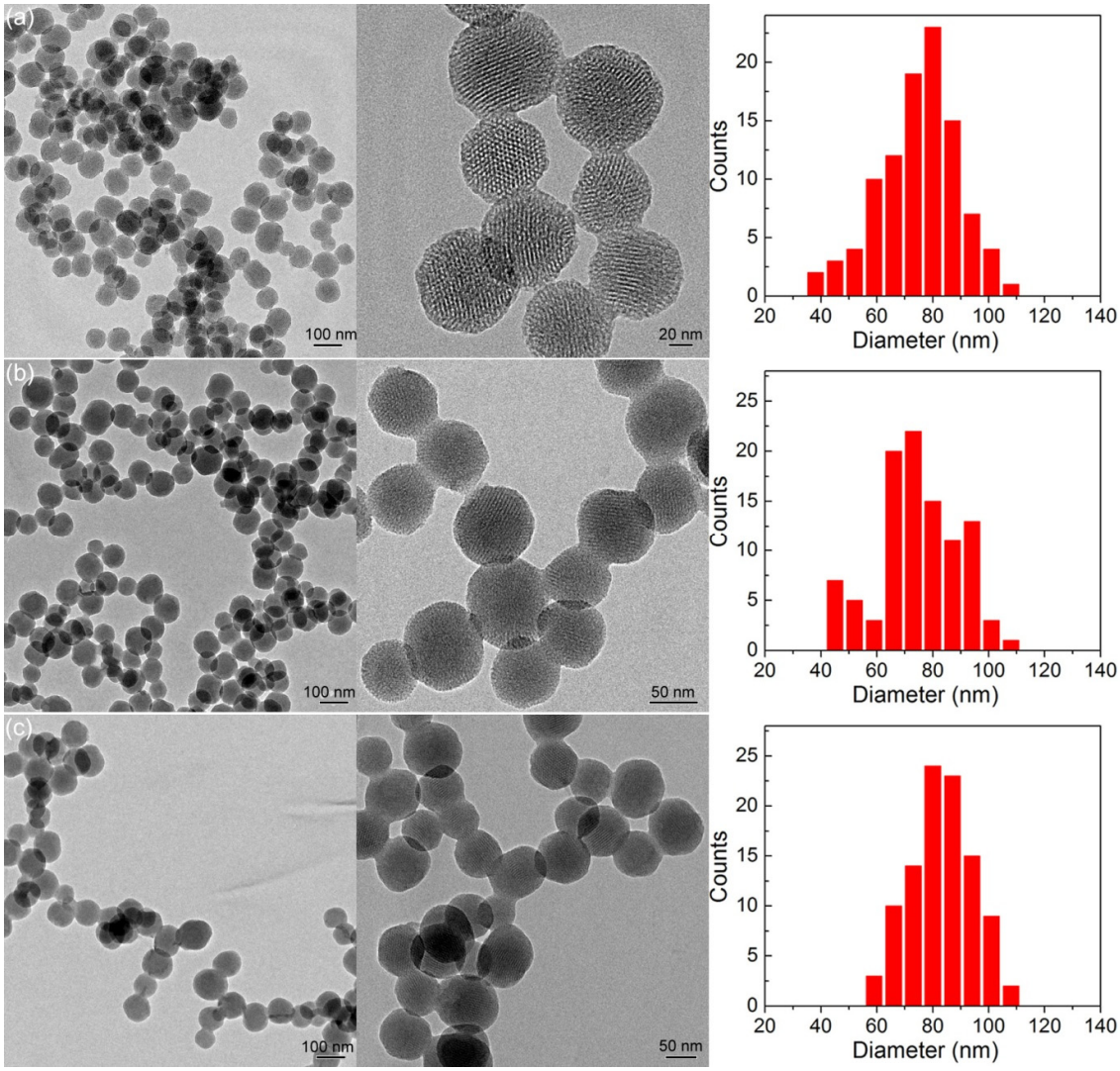
(a)
100 nm
20 nm
(b)
100 nm
50 nm
(c)
100 nm
50 nm
Counts
Diameter (nm)
0
5
10
15
20
25
20
40
60
80
100
120
140

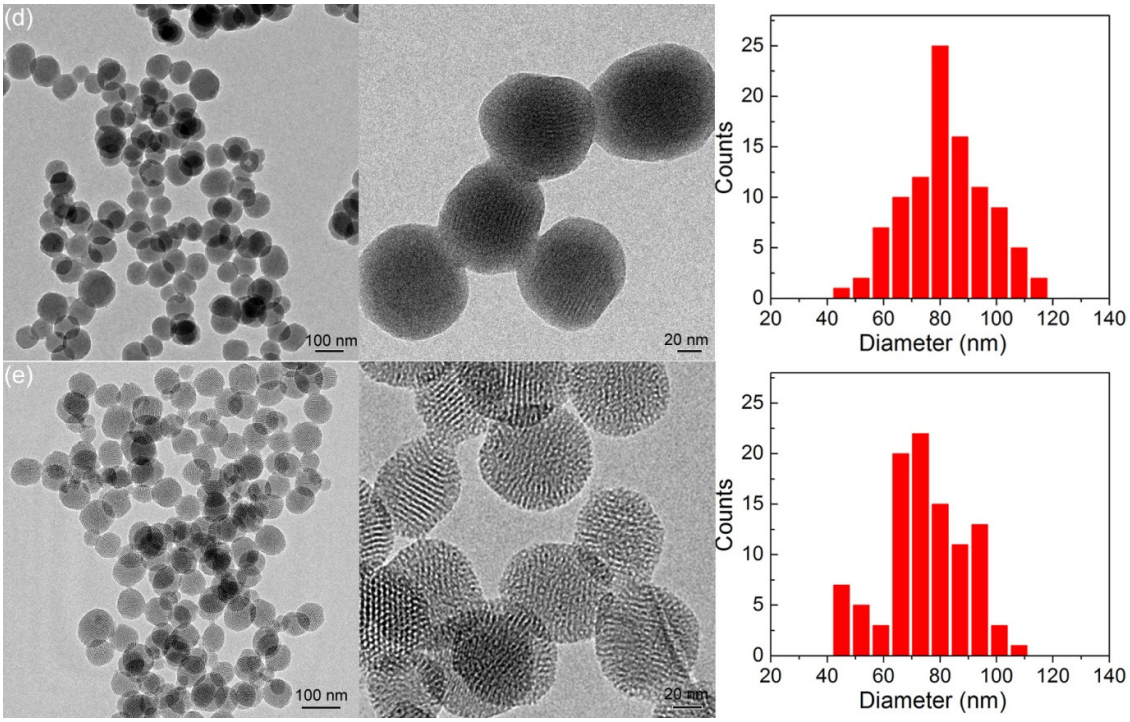

Fig. S1 TEM images of (a) A-MSN, (b) M-MSN, (c) Ph-MSN (d) T-MSN and (e) R-MSN. The hightograms at right show the particle size distribution of particles. The histograms were generated by measuring the diameter of 100 particles from the TEM images.

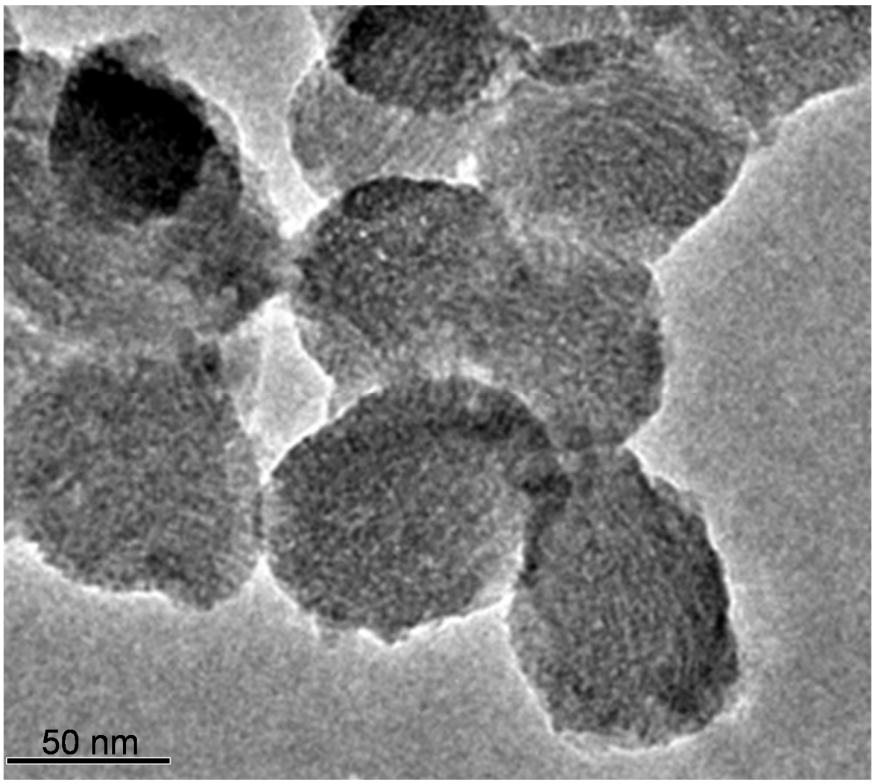

Fig. S2 TEM image of PEG-MSN. Thin organic layer formed around the particles can be observed from the TEM image.

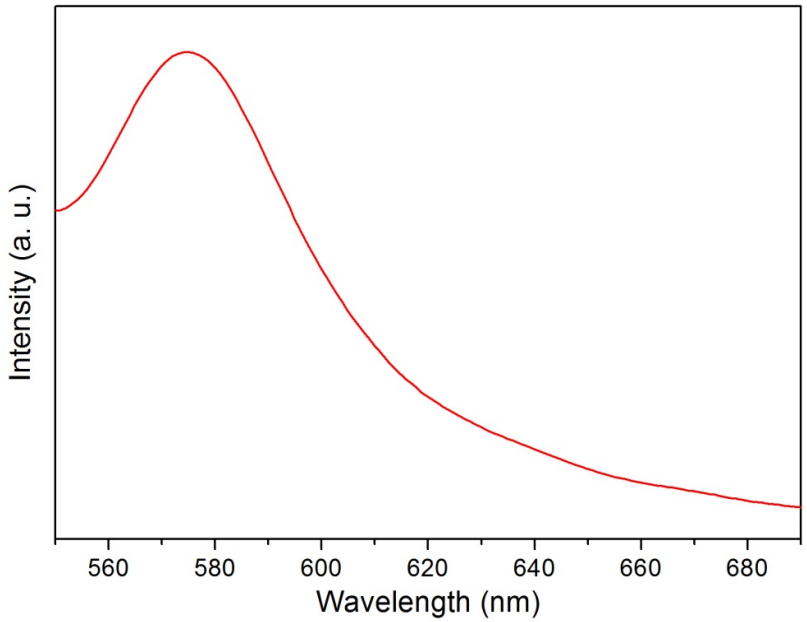

Fig. S3 Fluorescence spectrum of R-MSN. The bright fluorescence of Rhodamine B dye can be clearly seen.

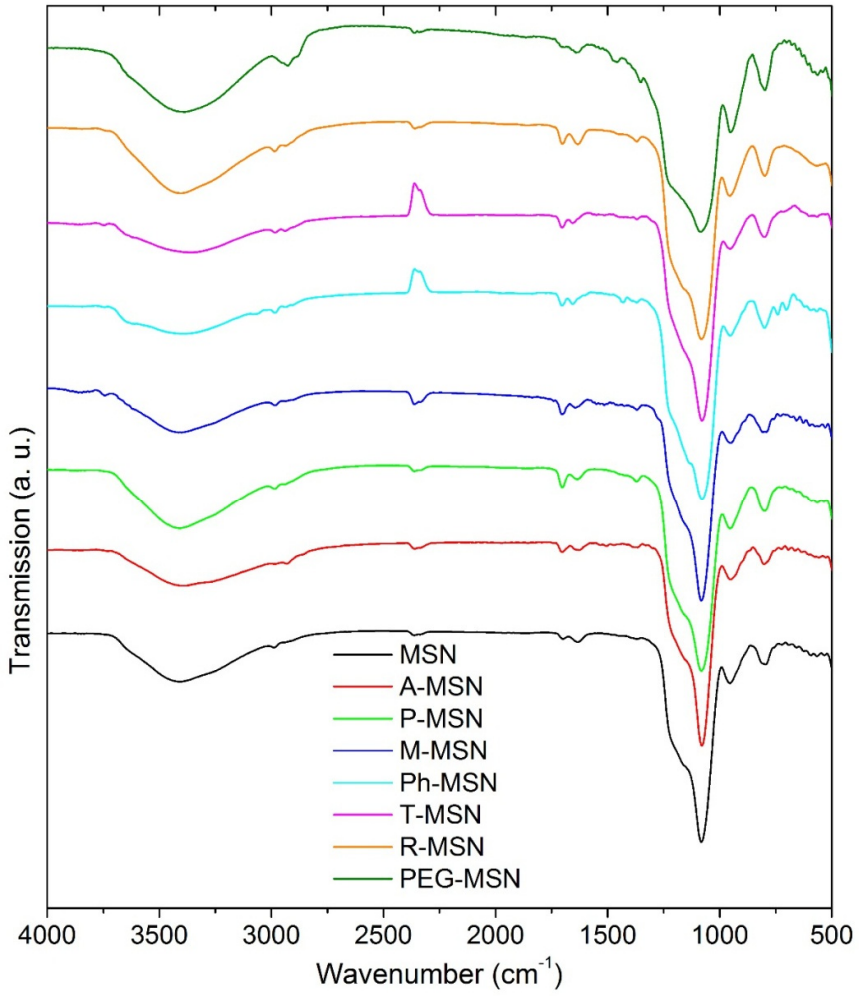

Fig. S4 FT-IR absorption spectra of all MSNs. The C-H absorption peak around 3000 cm^{-1} is more distinct for functionalized MSNs.

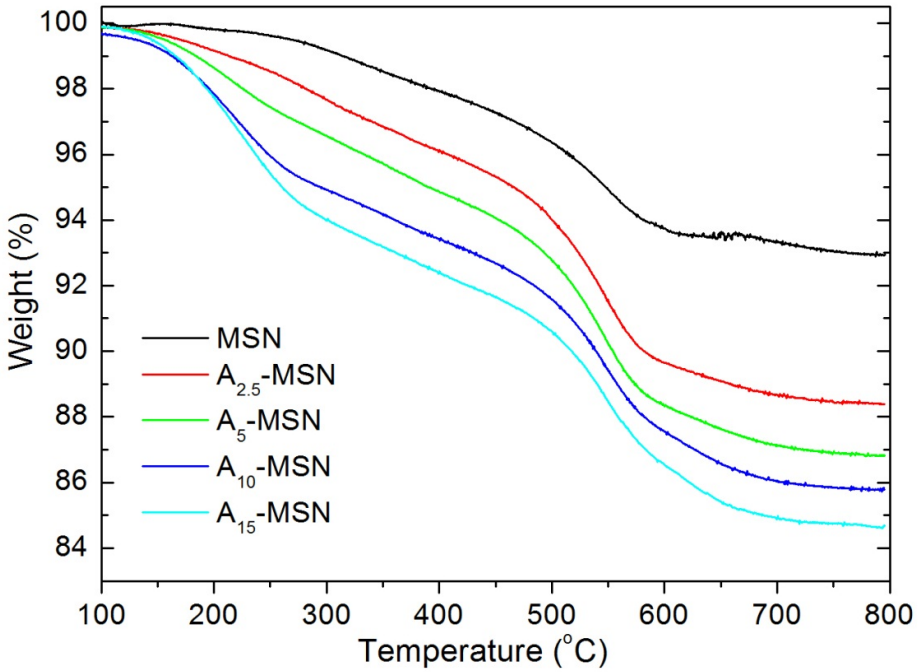

Fig. S5 TGA spectra of aminopropyl modified MSNs. As the APTES/TEOS molar percentages increased the weight loss also increased.

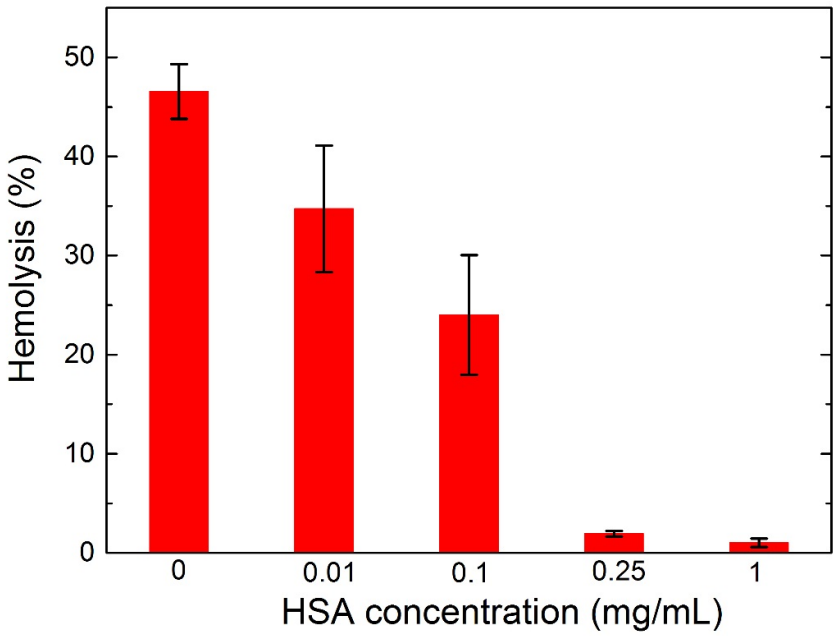

Fig. S6 Hemolysis results of HSA coated MSNs. With increasing HSA concentration reduced hemolytic activity was observed.